ROMANIAN JOURNAL OF INFORMATION SCIENCE AND TECHNOLOGY
Volume 28, Number 1, 2025, 77–88

Carbon Nano-Onions-Based Matrix Nanocomposite as Sensing Film for Resistive Humidity Sensor

Bogdan-Catalin SERBAN[1, *], Niculae DUMBRAVESCU[1], Octavian BUIU[1], Marius BUMBAC[2,3], Mihai BREZEANU[4], Cristina PACHIU[1], Cristina-Mihaela NICOLESCU[3], Cornel COBIANU[5], Cosmin ROMANITAN[1], and Vasilica TUCUREANU[1]

[1]National Institute for Research and Development in Microtechnologies, IMT-Bucharest, 126 A Str. Erou Iancu Nicolae, 077190, Voluntari, Ilfov, Romania

[2]Valahia University of Târgoviște, Faculty of Sciences and Arts, Sciences and Advanced Technologies Department, Aleea Sinaia, nr 13, 130004, Târgoviște, Dâmbovița, Romania

[3]Valahia University of Târgoviște, Institute of Multidisciplinary Research for Science Technology, Aleea Sinaia, nr 13, 130004, Târgoviște, Dâmbovița, Romania

[4]Faculty of Electronics, Telecommunications and IT, National University of Science and Technology Politehnica Bucharest, Bd Iuliu Maniu 1-3, 061071, Bucharest, Romania

[5]eBio-hub Center of Excellence in Bioengineering, National University of Science and Technology Politehnica Bucharest, Blvd. Iuliu Maniu Nr. 6, Sector 6, Bucharest 061344, Bucharest, Romania

Email: bogdan.serban@imt.ro*, niculae.dumbravescu@imt.ro octavian.buiu@imt.ro, marius.bumbac@valahia.ro, mbrezeanu@upb.ro, cristina.pachiu@imt.ro, cristina.nicolescu@valahia.ro, cornel.cobianu@gmail.com, cosmin.romanitan@imt.ro, vasilica.tucureanu@imt.ro*

* Corresponding author

Abstract. This paper reports several preliminary investigations concerning the relative humidity (RH) detection response of a chemiresistive sensor that uses a novel sensing film based on a matrix nanocomposite comprising pristine carbon nano-onions and polyvinylpyrrolidone polymer at 1/1 w/w. The sensing device, including a polyimide substrate and gold electrodes, is obtained by depositing by drop casting the sensing layer on the sensing structure. The sensing layer's morphology and composition are analyzed by Scanning Electron Microscopy, Atomic Force Microscopy, Fourier Transform Infrared Spectroscopy, X-Ray diffraction, and Raman spectroscopy. The experimental measurements show that the resistance of the tested nanocomposite slightly increases with RH for RH ¡ 50% and has a sharp increase with RH for larger RH. Several types of possible RH sensing mechanisms are identified and discussed. The decrease of the hole concentration in the CNOs in interaction with

water molecules, which act as electron donors, and the rapid swelling of the hydrophilic polyvinylpyrrolidone polymer at high RH levels are the RH sensing mechanisms that best explain the measured RH detection behavior. The hard–soft acid–base principle also supports the experimental data. The hysteresis characteristic of the sensor is improved after the first operating cycle.

Key-words: Carbon nano-onions; Hard Soft Acid Base theory; polyvinylpyrrolidone; resistive relative humidity sensor; swelling.

1. Introduction

Carbon nano-onions (CNOs), also called carbon-onions or onion-like carbon (OLC), are a type of carbon nanomaterial that includes quasi-spherical graphic layers positioned close to one another. Structurally, CNOs may be classified as multi-shell fullerenes (allotropes of carbons), including a hollow internal core surrounded by concentric graphene sheets [1]. Iijima et al. were the first to observe onion-like nanostructures in 1980 in synthesized amorphous carbon films following a vacuum evaporation process [2]. Ugarte was the first to synthesize these carbonaceous structures by electron irradiation of carbon soot particles in 1992 [3]. CNOs have high thermal stability, average electrical conductivity, relatively high surface-to-volume ratio, low friction coefficient, high mesoporosity, excellent corrosion resistance, high thermal stability, controlled size distribution, low level of toxicity, and good compatibility for being employed in matrix nanocomposites and hybrids [4]. Given these physicochemical properties, CNOs were used in various areas: manufacture of lubricants [5], electronics [6], broadband optical limiters [7], Li-ion-based electrochemical energy-storage devices [8], environmental monitoring [9], electrocatalysis [10], gas storage [11], nanocarriers for drug delivery [12], dye-sensitized solar cells [13], supercapacitors [14] etc. At the same time, CNOs were employed in chemical sensors and biosensors [15]. Measurands such as acetone, methanol, ethanol, and ammonia were reported to be detected using as sensing layers within structures of resistive sensors, pristine and doped CNOs, and their derivatives [16]. Materials based on CNOs were also used as sensing layers in the gravimetric detection of formaldehyde [17] and H2S [18]. The versatile covalent and noncovalent functionalization of CNOs enables the efficient synthesis of compounds with high sensitivity to specific target measurands. For instance, oxidation of CNOs using dilute nitric acid or ozone results in onion-like nanocarbon structures functionalized with hydrophilic groups such as carboxyl, hydroxyl, and carbonyl [19]. Resistive sensors using these functionalized structures have been shown to detect relative humidity (RH) [20]. This paper reports on the RH detection response of a chemiresistive sensing structure based on a novel sensing layer consisting of a matrix of nanocomposites, including pristine CNOs and polyvinylpyrrolidone (PVP) at 1/1 w/w. The paper is structured as follows: sensing layer synthesis and sensing structure layout are presented in Section 2, sensing layer characterization, experimental RH response of the sensing structure, and possible RH sensing mechanisms are presented and discussed in Section 3, while Section 4 is dedicated to conclusions sequentially.

2. Experimental

CNOs used for the RH measurements were purchased from Shanghai Epoch Material Co. Ltd and had diameters in the 5 nm - 8 nm range (Fig. 1a). All additional materials utilized in the experimental work were procured from Sigma Aldrich. PVP with an average molecular weight of 10,000 Da was used (Fig. 1b). Dimethylformamide ($(CH_3)_2N$-CHO, ACS reagent, $\geq$99.8%) was also employed. All chemicals were used as purchased without additional treatment.

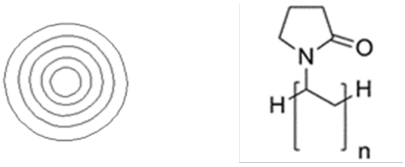

Fig. 1. Structure of: a) CNOs, and b) PVP.

The sensing layer, composed of the CNOs-PVP matrix nanocomposite, with a 1:1 mass ratio (w/w), was synthesized as follows: first, a PVP solution was prepared by dissolving 3 mg of PVP in 15 mL of dimethylformamide. This solution was sonicated in an ultrasonic bath (FS20D Fisher Scientific, Germany) operating at 42 kHz with a 70 MW output power for 30 minutes. Subsequently, 3 mg of CNOs were added to the solution and dispersed via ultrasonic agitation for 6 hours at room temperature (RT). The resulting dispersion was drop-cast onto a polyimide

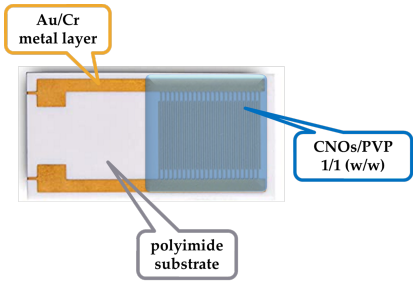

Fig. 2. Layout of IDT sensing structure (area: 5x7 mm^2).

substrate equipped with gold electrodes in an interdigital transducer (IDT) configuration (Fig. 2). The deposited layer was heated at 80°C for 3 hours under vacuum, then dried at 100°C for 1 hour. This is the first report on the synthesis of a sensing layer comprising CNOs and PVP.

To evaluate its RH detection performance, the proposed resistive sensing device including the novel sensing layer (sensor under test – SUT), utilizing the CNOs-PVP nanocomposite as detection layer, was tested alongside a commercial capacitive RH sensor (SENS) serving as a reference [21]. Both sensors were placed inside the testing box shown in Fig. 3.

In the experimental setup, dry nitrogen was passed through bubblers containing deionized water to achieve RH variations within the 0%–100% range. Digital mass flow controllers (MFCs) were used to mix dry and wet nitrogen in varying ratios. Before measurements, the sensors were exposed to dry nitrogen for 10 hours to ensure an anhydrous environment. Both SENS and the SUT were positioned near the gas inlet, thus ensuring they experienced similar gas flow and

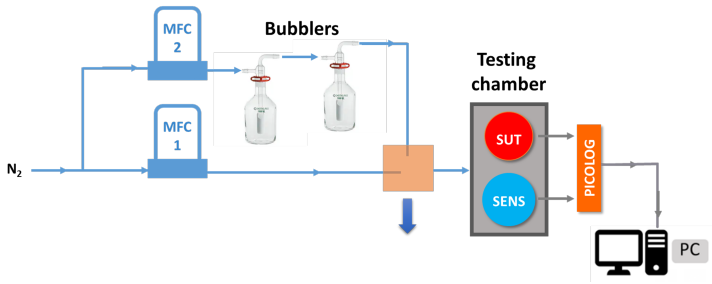

Fig. 3. Experimental setup for the RH detection.

quasi-similar experimental conditions [22]. Electric current variations in the 0.01–0.1 A range were generated using a Keithley 6620 DC current source. The output voltage was recorded, and electrical resistance was calculated using a PicoLog data logger. The total electrical power consumption of the chemiresistive sensor employing the novel sensing layer was measured to be less than 2 mW, offering a significant advantage over comparable RH sensors. The low power consumption is attributed to operating the sensor at RT, and it is consistent with the behavior of other sensors reported in the literature [23].

3. Results and discussions

The chemical bonds configuration of the CNOs-PVP nanocomposite was analyzed by means of Fourier Transform Infrared Spectroscopy (FTIR) (Fig. 4), performed at RT, using a Bruker Tensor 27 spectrometer, in the 4,000–370 cm^{-1} wavenumber domain, by averaging 64 scans and with 4 cm^{-1} resolution.

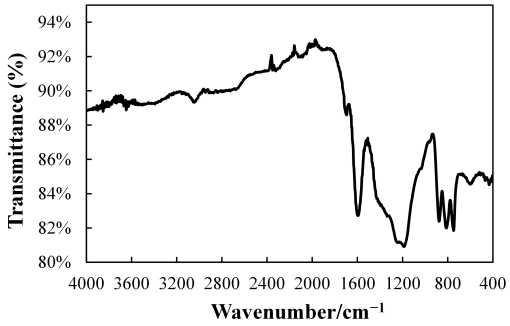

Fig. 4. Transmittance spectrometry of the CNOs-PVP nanocomposite material as a function of wavenumber.

Typically, the broad vibration peak between 3,000 and 3,500 cm^{-1} is associated with the OH groups. However, in this case, the peaks of reduced intensity in the range of 4,000-3,400 cm^{-1} are probably due to the OH groups adsorbed by the CNOs during handling. The vibration at 1696 cm^{-1} represents the C=O carbonyl group. The vibration at 1,594 cm^{-1} corresponds to C=C stretching due to aromatic rings or an alkene functional group, while the vibration at 1,187

cm^{-1} corresponds to C-C bonds. The morphology and composition of the RH detection layer were analyzed through structural characterization by scanning electron microscopy (SEM) images, which have revealed the presence of agglomerated CNOs-PVP structures, with a maximum particle size of 1-3 µm. (Fig.5).

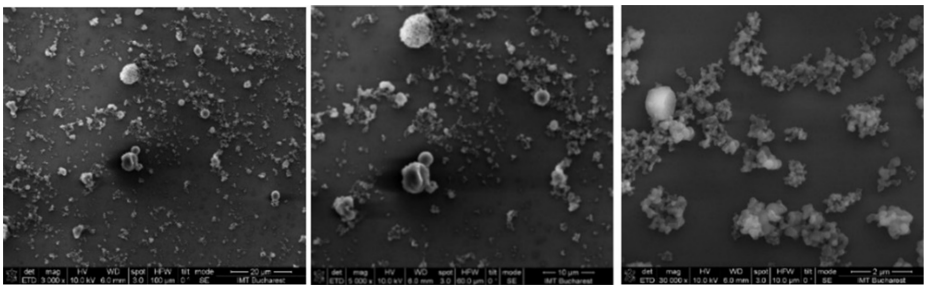

Fig. 5. SEM of the CNOs-PVP RH sensing layer at x 3,000 magnification (left), x 5,000 magnification (center), x 30,000 magnification (right).

Atomic force microscopy (AFM) analysis (Fig. 6) was conducted using a WITec Scanning Near-field Optical Microscope operating in the tapping mode. The analysis employed a Si_3N_4 AFM cantilever with a length of 125 μm, a force constant of 40 N/m, and a frequency of 300 kHz. The surface parameters were calculated using Project FIVE 5.0 Witec software.

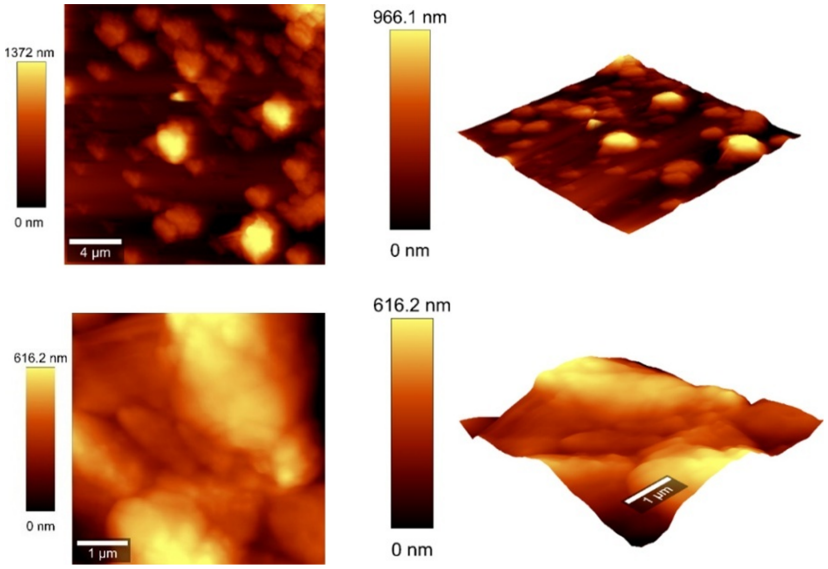

Fig. 6. AFM images of the CNOs-PVP RH sensing layer: Image 1 - SQ = 265.4 nm (top left) and associated SQ (root mean square roughness – top right), Image 2 - SQ = 265.4 nm (bottom left) and associated SQ (bottom right).

Raman spectroscopy analysis was performed to characterize the RH sensing layer. The Raman spectra were obtained at RT using a WITec Scanning Near-field Optical Microscope equipped with a 532 nm diode-pumped solid-state laser delivering 145 mW of power. The laser

beam, with a spot size of approximately 1.0 μm, was focused on the RH sensing sample using a 6 mm working distance objective mounted on a Thorlabs MY100X-806 microscope. The spectra were recorded with an exposure time of 20 seconds per accumulation, and scattered light was collected in a back-scattering geometry through the same objective, using 600 grooves/mm grating. Calibration of the Raman system was conducted using the 520 cm^{-1} Raman peak of silicon. The data acquisition and processing were performed using WiTec Project Five software (Version 5.1). The Raman spectrum showed two prominent peaks at 1,332 cm^{-1} and 1,586 cm^{-1}, corresponding to the defects, D and graphene, G bands, respectively, and a weaker peak at 2,672 cm^{-1}, associated with the 2D band, all specific to carbonic nanomaterials (Fig. 7) [24]. Additionally, a weak band at 2,990 cm^{-1} was attributed to PVP.

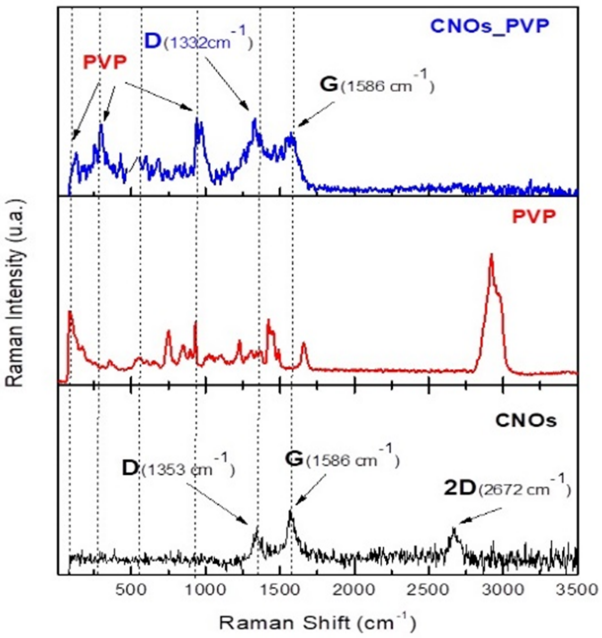

Fig. 7. Raman spectra of the solid-state film of the CNOs-PVP 1/1 (w/w) RH sensing layer deposited on the polyimide substrate.

The microstructure of the analyzed RH sensing sample was also examined by means of X-ray diffraction. For this purpose, an X-ray diffractometer with a nominal power of 9 kW (Rigaku SmartLab) was employed. A $\theta/2\theta$ configuration was used for the analysis of both the CNOs powder and the synthesized CNOs-PVP nanocomposite deposited on a Si substrate, a distinct structure from the RH sensing structure employed in the rest of the paper. The latter sample was analyzed at a sharp angle to minimize, as much as possible, the signal from the Si substrate.

Fig. 8 presents the diffractograms for the CNOs powder and the CNOs-PVP nanocomposite deposited on the Si substrate. For the CNOs powder, a prominent diffraction peak is observed at 23.2°, along with secondary reflections at 2θ = 42.3°and 44.6°. The broadness of the main peak suggests the semi-crystalline nature of the carbon. Additionally, the weak peaks around 42°and 45°point to the disordered structure of the graphene rings within the CNOs, in agreement with

the rather reduced height of G peak with respect to D peak from the Raman spectra of CNO PVP nanocomposite in Fig. 7.

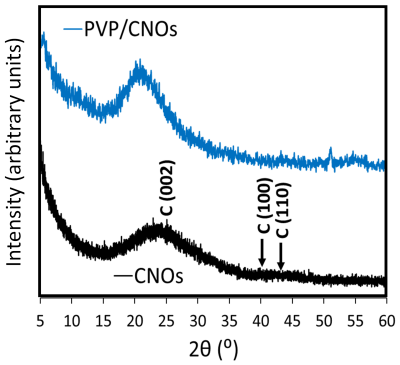

Fig. 8. X-ray diffractograms of 2 investigated samples: CNOs powder and the PVP-CNOs nanocomposite deposited on a Si substrate.

These findings are consistent with other studies on the microstructure of CNOs-based composites [25]. In the case of the CNOs-PVP nanocomposite deposited on the Si substrate, only a broad band is observed between approximately 15°and 25°, which is correlated with the semi-crystalline nature of pure PVP [26]. The RH sensing performance of the SUT at room temperature was evaluated by applying a continuous flow of the DC electric current between the electrodes and measuring the potential difference as the RH was varied from 0% to 100%. Measurements taken over three operating cycles (Fig. 9) demonstrated that the resistance of the SUT increased with RH across the entire RH range. For RH values below 55%, the resistance variation was linear, with a specific slope, while for RH values above 55%, the slope became significantly steeper. The relatively low electrical resistances measured at room temperature can be attributed to the composition of the CNOs-PVP sensing layer since the concentration of CNOs in the RH sensing film exceeds the percolation threshold of the carbon nanomaterial within the dielectric PVP matrix [27]. As a result, continuous conductive carbon paths are formed between the two metal electrodes of the RH sensor, leading to its low and easily measurable electrical resistance.

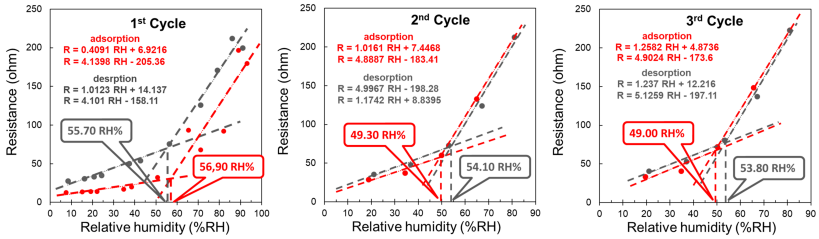

Fig. 9. Electrical resistance versus RH for SUT for the: a)1st, b) 2nd, and c) 3rd operating cycle (adsorption in red, desorption in grey).

The experimental RH detection results obtained for the SUT can be discussed and analyzed by considering and examining various RH sensing mechanisms. Firstly, it is important to note that CNOs are p-type semiconducting materials [28]. When water molecules come into

contact with the CNOs, they donate electron pairs, which reduces the hole concentration in the carbonaceous structure. As a result, the resistance of the entire sensing layer increases. Additionally, the interaction between water molecules and CNOs can be examined through the Hard and Soft Acid and Base (HSAB) principle [29]. Like other chemical species such as alcohols, alkoxides, ethers, hydrazine, and amines (primary, secondary, and tertiary), water molecules are considered hard bases due to their available electron pairs. The holes in the CNOs structure can be viewed as hard acids [30]. Given this, the interaction between water molecules and CNOs is highly plausible [31] and appears to be the dominant sensing mechanism for RH values below 55% during the first operating cycle. This RH threshold shifts to approximately 50% in subsequent cycles. As mentioned above, a much stronger correlation between the sensing layer resistance and RH was observed for RH values above the threshold. This phenomenon may be attributed to the swelling of PVP when it interacts with water molecules (Fig. 10). As PVP swells within the CNOs-PVP matrix nanocomposite, the number of contact points between the CNOs rapidly decreases. As a result, the number of conductive (percolative) carbon paths diminishes, leading to a sharp increase in the resistance of the sensing layer. This switch-like behavior of the CNOs-PVP matrix, where the resistance versus RH relationship shifts from one slope to another, is consistent with other reported findings [32].

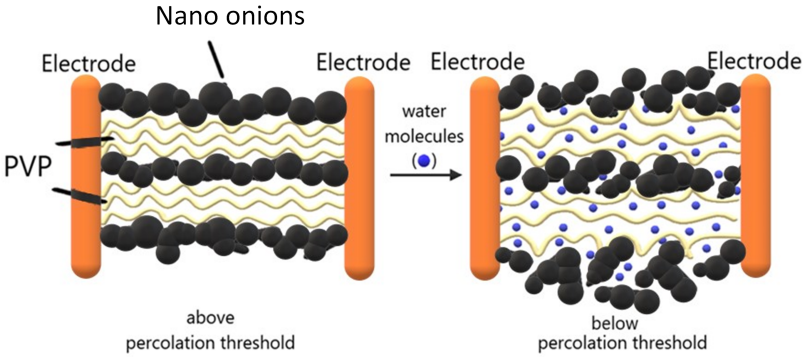

Fig. 10. The swelling of PVP upon contact with water molecules disrupts the percolating pathways of the CNOs.

Fig. 9a illustrates the first adsorption-desorption cycle. Comparing the data in Fig. 9a-c, it is evident that the measurements from the first cycle do not align with those from the second and third cycles. Additionally, the sensor's response is reproducible in the second and third cycles, with resistance variations of ±5% between cycles. The differences between the adsorption and desorption curves are minimal in comparison to the first cycle of RH measurements. The slope of the transfer functions in Figs. 9a-c can be related to the sensor's sensitivity, S, which is defined as the ratio of the resistance change (ΔR) to the RH change (ΔRH), as expressed by the equation (1):

$$S = \frac{\Delta R}{\Delta R_H} \tag{1}$$

The sensitivity of SUT triples once RH exceeds 50%. The inflection points, which signify the change in the sensor's behavior at higher RH levels, are clearly marked in Fig. 9a-c.

Apart from the 3 mechanisms described above, other RH detection mechanisms for CNOs were reported in the literature. For instance, it is suggested that, for RH ¿ 27.9%, CNOs move from p-type to n-type semiconducting behavior [16], which results in a decrease in resistance as RH increases. However, this behavior was not observed in the case of the RH detection measurements performed on SUT and described in this paper. Even if this phenomenon did occur, the significant swelling of the PVP in contact with water likely had a much more substantial impact on the RH detection than any potential change in the semiconducting properties of the CNOs. Additionally, the dissociation of water at high RH levels into H^+ and OH^- ions at the surface of the CNOs should also be considered, at least theoretically, when discussing the RH detection mechanism. The protons generated by the self-ionization of water could potentially hop between water molecules via hydrogen bonding, thereby decreasing the overall electrical resistance of the thin film. However, while this is also a plausible scenario, it is clear that measured RH detection characteristics show that proton conduction does not play a dominant role in chemiresistive RH sensing. It is also worth noting that the hysteresis in the resistance versus RH characteristic of the SUT significantly improved after the first operating cycle. One possible explanation is that, during the first cycle, the absorption of water molecules was followed by partial diffusion into the bulk of the sensing layer, allowing the water to condense in the capillaries (remanent water). As a result, water molecules adsorbed at the edges of the CNOs could be quickly released during desorption. This caused a significant difference between the humidification and dehumidification phases in the first cycle. From the second cycle onwards, the sensing film became stabilized, leading to a reduction in hysteresis.

4. Conclusions

This paper reports on the relative humidity sensing properties of a room temperate operated chemiresistive sensor, employing, as a novel sensing layer, a binary nanocomposite comprising CNOs and PVP at 1/1 (w/w), which was synthesized for the first time. The RH monitoring capability of the sensing structure was investigated by applying a continuous flow of DC electric current between the electrodes of the proposed sensor and measuring the voltage when varying RH in the range 0% - 100%. For RH lower than 55%, in the first operating cycle, the sensor's electrical resistance had a linear increase with RH, with a certain slope; for RH¿ 55%, the slope significantly increased. The measured behavior was similar for the following operating cycles, but the threshold value for changing the slope was lower: around 50%. The hysteresis of the resistance versus RH characteristic was significantly reduced after the first operating cycle. Different mechanisms for explaining the RH detection behavior of the analyzed sensing structure were considered and assessed. Based on the experimental results, it was argued that the p-type semiconductor behavior of CNOs in conjunction with the swelling of PVP in the presence of water prevailed and led to an overall increase in the sensing film electrical resistance with RH. The HSAB theory was also shown to support the experimental data. The key advantages of the proposed sensing structure include low power consumption (below 2 mW), excellent RH sensing performance at room temperature, and ease of fabrication. This detector could be highly valuable for future low-power sensors, particularly for Internet of Things (IoT) applications.

Acknowledgement. The authors from IMT Bucharest would like to acknowledge the financial support of Contract No. 673 PED/2022 (PN-III-P2-2.1-PED-2021-4158) – UEFISCDI.

References

[1] O.MYKHAILIV, H.ZUBYK and M.-E. PLONSKA BREZINSKA, *Carbon nano-onions: Unique carbon nanostructures with fascinating properties and their potential applications*, Inorganica Chimica Acta **468**, 2017, pp. 49–66.

[2] S. IIJIMA, *Direct observation of the tetrahedral bonding in graphitized carbon black by high resolution electron microscopy*, Journal of Crystal Growth **50**(3), 1980, pp. 675–683.

[3] D. UGARTE, *Curling and closure of graphitic networks under electron-beam irradiation*, Nature **359**, 1992, pp. 707–709.

[4] M. GHALKHANI, E.-M. KHOSROWSHAHI and E. SOHOULI, *Carbon nano-onions: Synthesis, characterization, and application*, Handbook of Carbon-Based Nanomaterials, Elsevier, 2021, pp. 159–207.

[5] A. HIRATA, M. IGARASHI and T. KAITO, *Study on solid lubricant properties of carbon onions produced by heat treatment of diamond clusters or particles*, Tribology International **37**(11–12), 2004, pp. 899–905.

[6] S. SEK, J. BRECZKO, M.-E. PLONSKA-BREZINSKA, A.-Z. WILCZEWSKA and L. ECHEGOYEN, *STM-based molecular junction of carbon nano-onion*, ChemPhysChem **14**, 2013, pp. 96–100.

[7] V. GEORGAKILAS, M.-D. GULDI, R. SIGNORINI, R. BOZIO and M. PRATO, *Organic functionalization and optical properties of carbon onions*, Journal of the American Chemical Society **125**(47), 2003, pp. 14268-14269.

[8] Q. WANG, X. SUN, D. HE and J. ZHANG, *Preparation and study of carbon nano-onion for lithium storage*, Materials Chemistry and Physics **139**(1), 2013, pp. 333–337.

[9] C. SAKULTHAEW, C. CHOKEJAROENRAT, A. POAPOLATHEP, T. SATAPANAJARU and S. POAPOLATHEP, *Hexavalent chromium adsorption from aqueous solution using carbon nano-onions (CNOs)*, Chemosphere **184**, 2017, pp. 1168–1174.

[10] O. MYKHAILIV, H. ZUBYK, K. BREZINSKI, M. GRAS, G. LOTA, M. GNIADEK and M.-E. PLONSKA BRZEZINSKA, *Improvement of the structural and chemical properties of carbon nano-onions for electrocatalysis*, ChemNanoMat **3**(8), 2017, pp. 583–590.

[11] S. SAHU, M.-S. KHAN, N. GUPTA, K. CHENNAKESAYULU and C. SASIKUMAR, *The hydrogen storage capacity of carbon nano-onions fabricated by thermal chemical vapour deposition*, International Journal of Hydrogen Energy **52**, 2024, pp. 1371–1383.

[12] M. BARTKOWSKI and S. GIORDANI, *Carbon nano-onions as potential nanocarriers for drug delivery*, Dalton Transactions **50**(7), 2021, pp. 2300–2309.

[13] B. PANG, M. ZHANG, C. ZHOU, H. DONG, S. MA, Y. SHI and L. DONG, *Nitrogen-doped carbon nano-onions decorated on graphene network: A novel all-carbon composite counter electrode for dye-sensitized solar cell with a 10.28% power conversion efficiency*, Solar RRL **4**(9), 2020, paper 2000263.

[14] S. KAUR, A. KRISHNAN and S. CHAKRABORTY, *Recent advances and challenges of carbon nano onions (CNOs) for application in supercapacitor devices (SCDs)*, Journal of Energy Storage **71**, 2023, paper 107928.

[15] E. SOHOULI, F. SHAHDOST-FARD, M. RAHIMI-NASRABADI, M.-E. PLONSKA-BRZEZINSKA and F. AHMADI, *Introducing a novel nanocomposite consisting of nitrogen-doped carbon nano-onions and gold nanoparticles for the electrochemical sensor to measure acetaminophen*, Journal of Electroanalytical Chemistry **871**, 2020, paper 114309.

[16] B.-P. DHONGE, D.-E. MOTAUNG, C.-P. LIU, Y.-C. LI and B. WMWAKIKUNGA, *Nano-scale carbon onions produced by laser photolysis of toluene for detection of optical, humidity, acetone, methanol and ethanol stimuli*, Sensors and Actuators B: Chemical **215**, 2015, pp. 30–38.

[17] B.-C. SERBAN, O. BUIU and V. DIACONESCU, *Carbon nanoonions-based nanohybrid for formaldehyde resistive detection*, Proceedings of 2024 International European Conference on Interdisciplinary Scientific Research, Universitat de Valencia, Valencia, Spain, 2024, paper 184.

[18] B.-C. SERBAN, O. BUIU and M. BUMBAC, *Thiolated carbon nanoonions as sensing layer for resistive hydrogen sulphide sensor*, Proceedings of 2023 International Architectural Sciences & Applications Symposium, Naples, Italy, 2023, paper 195.

[19] B.-C. SERBAN, O. BUIU, M. BUMBAC and C.-M. NICOLESCU, *Oxidated carbon nano-onions based ternary nanohybrid as sensing element for resistive humidity sensor*, Proceedings of 2023 International Paris Congress on Agriculture & Animal Husbandry, Paris, France, 2023, pp. 21–22.

[20] B.-C. SERBAN, O. BUIU, M. BUMBAC and C.-M. NICOLESCU, *Oxidated carbon nano-onions based matrix nanocomposite for novel resistive humidity sensor*, Proceedings of 2023 International Paris Congress on Agriculture & Animal Husbandry, Paris, France, 2023, pp. 23–24.

[21] B.-C. SERBAN, O. BUIU, N. DUMBRAVESCU, C. COBIANU, V. AVRAMESCU, M. BREZEANU, M. BUMBAC and C.-M. NICOLESCU, *Oxidized Carbon Nanohorns as Novel Sensing Layer for Resistive Humidity Sensor*, Acta Chimica Slovenica **67**(2), 2020, pp. 469–475.

[22] B.-C. SERBAN, C. COBIANU, O. BUIU, M. BUMBAC, N. DUMBRAVESCU, V. AVRAMESCU, C.-M. NICOLESCU, M. BREZEANU, C. RADULESCU, G. CRACIUN, C. ROMANITAN and F.-C. COMANESCU, *Quaternary Holey Carbon Nanohorns/SnO2/ZnO/PVP Nano-Hybrid as Sensing Element for Resistive-Type Humidity Sensor*, Coatings **11**(11), 2021, paper 1307.

[23] B.-C. SERBAN, C. COBIANU, N. DUMBRAVESCU, O. BUIU, V. AVRAMESCU, M. BUMBAC and C.-M. NICOLESCU, *Electrical percolation threshold in oxidized single wall carbon nanohorn-polyvinylpyrrolidone nanocomposite: A possible application for high sensitivity resistive humidity sensor*, Proceedings of 2020 International Semiconductor Conference, Sinaia, Romania, 2020, pp. 239–242.

[24] B.-C. SERBAN, N. DUMBRAVESCU, O. BUIU, M. BUMBAC, M. BREZEANU, C. PACHIU and V. DIACONESCU, *Resistive humidity sensor based on Onion-like Carbon-PVA composite sensing film*, Proceedings of 2024 IEEE International Semiconductor Conference, Sinaia, Romania, 2024, pp. 65–68.

[25] V. DHAND, J. SARADA PRASAD, M. VENKATESWARA RAO, S. BHARADWAJ, Y. ANJANEYULU and P.-K. JAIN, *Flame synthesis of carbon nano onions using liquefied petroleum gas without catalyst*, Materials Science and Engineering: C **33**(2), 2013, pp. 758–762.

[26] J. LV, W. GU, X. CUI, S. DAI, B. ZHANG and J.-I. GUANGBIN, *Nanofiber network with adjustable nanostructure controlled by PVP content for an excellent microwave absorption*, Scientific Reports **9**(1), 2019, paper 4271.

[27] B.-C. SERBAN, C. COBIANU, N. DUMBRAVESCU, O. BUIU, M. BUMBAC, C.-M. NICOLESCU, M. BREZEANU, C. PACHIU and M. SERBANESCU, *Electrical percolation threshold and size effects in Polyvinylpyrrolidone-Oxidized Single-Wall Carbon nanohorn nanocomposite: The impact for relative humidity resistive sensors design*, Sensors **21**, 2021, paper 1435.

[28] S.-D. LAWANIYA, S. KUMAR, Y. YU and K. AWASTHI, *Nitrogen-doped carbon nano-onions/polypyrrole nanocomposite based low-cost flexible sensor for room temperature ammonia detection*, Scientific Reports **14**(1), 2024, paper 7904.

[29] R. G. PEARSON, *The HSAB principle—more quantitative aspects*, Inorganica Chimica Acta **240**(1-2), 1995, pp. 93–98.

[30] C. COBIANU, B.-C. SERBAN, N. DUMBRAVESCU, O. BUIU, V. AVRAMESCU and C. PACHIU, *Organic–inorganic ternary nanohybrids of single-walled carbon nanohorns for room temperature chemiresistive ethanol detection*, Nanomaterials **10**(12), 2020, paper 2552.

[31] B.-C. SERBAN, M. BREZEANU, C. COBIANU, S. COSTEA, O. BUIU, A. STRATULAT and N. VARACHIU, *Materials selection for gas sensing. An HSAB perspective*, Proceedings of 2014 IEEE International Semiconductor Conference, Sinaia, Romania, 2014, pp. 21–30.

[32] B.-C. SERBAN, O. BUIU, N. DUMBRAVESCU, C. COBIANU, V. AVRAMESCU, M. BREZEANU, M. BUMBAC, C. PACHIU and C.-M. NICOLESCU, *Oxidized carbon nanohorn-hydrophilic polymer nanocomposite as the resistive sensing layer for relative humidity*, Analytical Letters **54**(3), 2021, pp. 527–540.